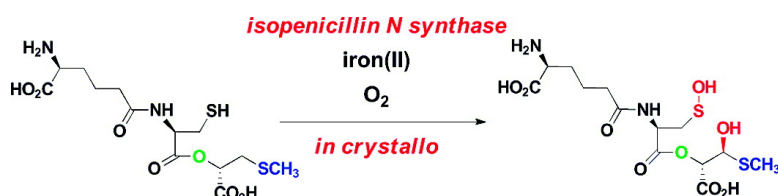


## Isopenicillin N Synthase Mediates Thiolate Oxidation to Sulfenate in a Depsipeptide Substrate Analogue: Implications for Oxygen Binding and a Link to Nitrile Hydratase?

Wei Ge, Ian J. Clifton, Jeanette E. Stok, Robert M. Adlington, Jack E. Baldwin, and Peter J. Rutledge

*J. Am. Chem. Soc.*, **2008**, 130 (31), 10096-10102 • DOI: 10.1021/ja8005397 • Publication Date (Web): 12 July 2008

Downloaded from <http://pubs.acs.org> on February 8, 2009



### More About This Article

Additional resources and features associated with this article are available within the HTML version:

- Supporting Information
- Access to high resolution figures
- Links to articles and content related to this article
- Copyright permission to reproduce figures and/or text from this article

[View the Full Text HTML](#)

## Isopenicillin N Synthase Mediates Thiolate Oxidation to Sulfenate in a Depsipeptide Substrate Analogue: Implications for Oxygen Binding and a Link to Nitrile Hydratase?

Wei Ge,<sup>‡</sup> Ian J. Clifton,<sup>‡</sup> Jeanette E. Stok,<sup>‡,‡</sup> Robert M. Adlington,<sup>‡</sup>  
Jack E. Baldwin,<sup>\*,‡</sup> and Peter J. Rutledge<sup>\*,§</sup>

Chemistry Research Laboratory, University of Oxford, Mansfield Road, Oxford, OX1 3TA, U.K.,  
and School of Chemistry F11, University of Sydney, NSW 2006, Australia

Received January 22, 2008; E-mail: p.rutledge@chem.usyd.edu.au; jack.baldwin@chem.ox.ac.uk

**Abstract:** Isopenicillin N synthase (IPNS) is a nonheme iron oxidase that catalyzes the central step in the biosynthesis of  $\beta$ -lactam antibiotics: oxidative cyclization of the linear tripeptide  $\delta$ -L- $\alpha$ -aminoadipoyl-L-cysteiny-D-valine (ACV) to isopenicillin N (IPN). The ACV analogue  $\delta$ -L- $\alpha$ -aminoadipoyl-L-cysteine (1-(S)-carboxy-2-thiomethyl)ethyl ester (ACOmC) has been synthesized as a mechanistic probe of IPNS catalysis and crystallized with the enzyme. The crystal structure of the anaerobic IPNS/Fe(II)/ACOmC complex was determined to 1.80 Å resolution, revealing a highly congested active site region. By exposing these anaerobically grown crystals to high-pressure oxygen gas, an unexpected sulfenate product has been observed, complexed to iron within the IPNS active site. A mechanism is proposed for formation of the sulfenate–iron complex, and it appears that ACOmC follows a different reaction pathway at the earliest stages of its reaction with IPNS. Thus it seems that oxygen (the cosubstrate) binds in a different site to that observed in previous studies with IPNS, displacing a water ligand from iron in the process. The iron-mediated conversion of metal-bound thiolate to sulfenate has not previously been observed in crystallographic studies with IPNS. This mode of reactivity is of particular interest when considered in the context of another family of nonheme iron enzymes, the nitrile hydratases, in which post-translational oxidation of two cysteine thiolates to sulfenic and sulfinic acids is essential for enzyme activity.

### Introduction

The linear tripeptide  $\delta$ -L- $\alpha$ -aminoadipoyl-L-cysteiny-D-valine (ACV) is converted to bicyclic isopenicillin N (IPN), biosynthetic precursor to all penicillins and cephalosporins) by a single enzyme, isopenicillin N synthase (IPNS).<sup>1,2</sup> The reaction stoichiometry involves the loss of four hydrogen atoms from ACV, concomitant with the reduction of one equivalent of molecular oxygen to two molecules of water.<sup>2</sup> On the basis of detailed spectroscopic investigation, incubation studies,<sup>3</sup> and crystallography experiments,<sup>4–6</sup> a detailed mechanism for the IPNS catalyzed conversion of ACV to IPN has been proposed.<sup>1,5,6</sup> The two rings of IPN are closed

sequentially: initial  $\beta$ -lactam formation gives rise to a reactive iron(IV)-oxo species which then mediates thiazolidine ring closure (Scheme 1).

Crystal structures of IPNS/Mn(II) and of the anaerobic substrate complexes IPNS/Fe(II)/ACV and IPNS/Fe(II)/ACV/NO (incorporating nitric oxide as a dioxygen analogue) were determined in the late 1990s.<sup>4,5</sup> More recently, we have developed a method for turnover experiments whereby an oxygen “bomb” was designed to expose crystals to dioxygen levels of up to 60 bar, promoting turnover within protein crystals.<sup>6,7</sup> High-pressure application of oxygen maximizes penetration of the gas through the crystals and consequently gives a high degree of simultaneous initiation of the reaction in the crystal.<sup>6</sup> Since the electron density map obtained from X-ray analysis is a superposition of all the structural states present in the crystal lattice at the time of data collection, homogeneity of the states present is required for accurate structural determination. This approach has allowed the structure of the natural enzyme–product complex to be elucidated and an array of valuable mechanistic information to be determined using a range of modified substrate analogues.<sup>6,8–16</sup> Such analogues are designed to contain

<sup>‡</sup> University of Oxford.

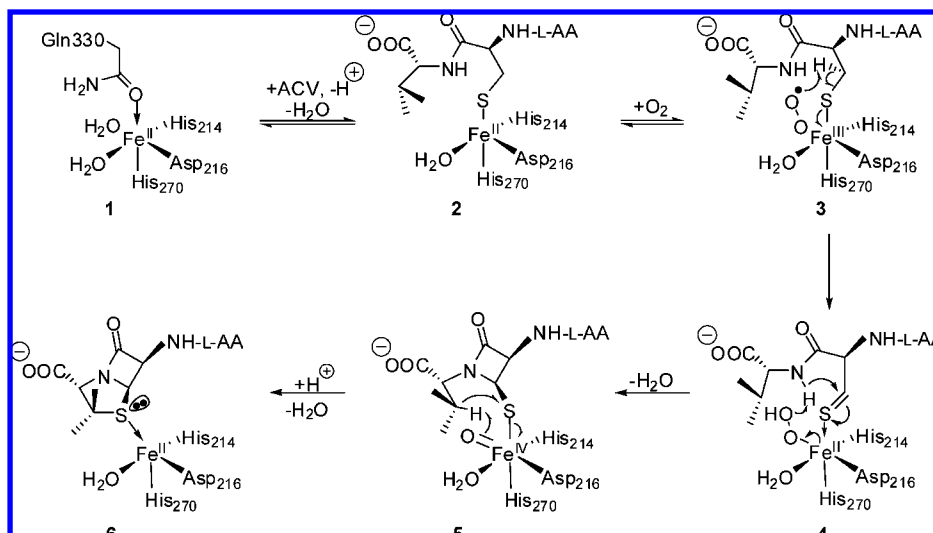
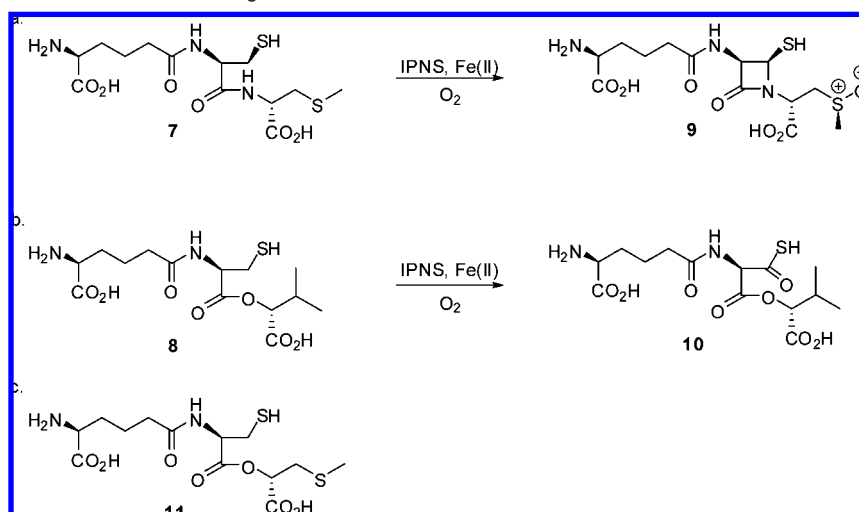
<sup>§</sup> University of Sydney.

<sup>†</sup> Current address: CBio Limited, P.O. Box 8104, Queensland 4109, Australia.

- (1) Baldwin, J. E. In *Special Publication No. 52*; Brown, A. G., Roberts, S. M., Eds.; The Royal Society of Chemistry: London, 1985; pp 62–85.
- (2) Baldwin, J. E.; Schofield, C. J. In *The Chemistry of  $\beta$ -Lactams*; Page, M. I., Ed.; Blackie: Glasgow, 1992; pp 1–78.
- (3) Baldwin, J. E.; Bradley, M. *Chem. Rev.* **1990**, *90*, 1079–1088.
- (4) Roach, P. L.; Clifton, I. J.; Fulop, V.; Harlos, K.; Barton, G. J.; Hajdu, J.; Andersson, I.; Schofield, C. J.; Baldwin, J. E. *Nature* **1995**, *375*, 700–704.
- (5) Roach, P. L.; Clifton, I. J.; Hensgens, C. M. H.; Shibata, N.; Schofield, C. J.; Hadju, J.; Baldwin, J. E. *Nature* **1997**, *387*, 827–830.
- (6) Burzlaff, N. I.; Rutledge, P. J.; Clifton, I. J.; Hensgens, C. M. H.; Pickford, M.; Adlington, R. M.; Roach, P. L.; Baldwin, J. E. *Nature* **1999**, *401*, 721–724.

(7) Rutledge, P. J.; Burzlaff, N. I.; Elkins, J. M.; Pickford, M.; Baldwin, J. E.; Roach, P. L. *Anal. Biochem.* **2002**, *308*, 265–268.

(8) Ogle, J. M.; Clifton, I. J.; Rutledge, P. J.; Elkins, J. M.; Burzlaff, N. I.; Adlington, R. M.; Roach, P. L.; Baldwin, J. E. *Chem. Biol.* **2001**, *8*, 1231–1237.

**Scheme 1.** Proposed Mechanism for Oxidative Cyclization of ACV to IPN<sup>5</sup>**Scheme 2.** Reaction of IPNS with Substrate Analogues ACmC **7** and AcOV **8**<sup>a</sup>

<sup>a</sup> (a) Turnover of ACmC in crystalline IPNS;<sup>6</sup> (b) reaction of ACOV in crystalline IPNS;<sup>8</sup> (c) structure of the new mechanistic probe ACOmC **11**.

chemical modifications so as to interrupt the reaction cycle at an intermediate stage.

Using this approach,  $\delta$ -(L- $\alpha$ -aminoadipoyl)-L-cysteiny-L-S-methyl-D-cysteine (ACmC, **7**)<sup>6</sup> and  $\delta$ -(L- $\alpha$ -aminoadipoyl)-L-cysteine D- $\alpha$ -hydroxyisovaleryl ester (ACOV, **8**)<sup>8</sup> were synthesized and crystallized with IPNS and Fe(II) under anaerobic conditions. These crystals were then exposed to high-pressure oxygenation to give turnover products (Scheme

2). ACmC **7** gave a monocyclic  $\beta$ -lactam **9**, providing firm structural evidence that  $\beta$ -lactam ring closure occurs prior to thiazolidine formation. ACOV produced the thio-carboxylic acid **10** *via* an alternative reaction pathway in which the proposed hydroperoxide intermediate appears to attack the putative thioaldehyde species directly (in the absence of its natural reaction partner, the NH of the Cys-Val amide link). This transformation involves removal of both hydrogen atoms from the cysteinyl  $\beta$ -carbon.

Based on these studies with ACmC **7** and ACOV **8**, the “hybrid” analogue  $\delta$ -L- $\alpha$ -aminoadipoyl-L-cysteine (1-(S)-carboxy-2-thiomethyl)ethyl ester **11** has been devised as a new chemical trap for a hydroperoxide type intermediate. (The substrate analogue **11** is referred to henceforth as (LLD)-ACOmC to highlight its structural relationships to the tripeptide ACmC **7** and depsipeptide ACOV **8**.) This analogue combines the S-methyl group of ACmC with the ester linkage of ACOV: like ACOV, ACOmC lacks the valinyl amide NH removed during  $\beta$ -lactam formation (and thus cannot form the  $\beta$ -lactam ring), and like ACmC, ACOmC includes the methyl sulfide to intercept the proposed hydroperoxide

- (9) Elkins, J. M.; Rutledge, P. J.; Burzlaff, N. I.; Clifton, I. J.; Adlington, R. M.; Roach, P. L.; Baldwin, J. E. *Org. Biomol. Chem.* **2003**, *1*, 1455–1460.
- (10) Long, A. J.; Clifton, I. J.; Roach, P. L.; Baldwin, J. E.; Schofield, C. J.; Rutledge, P. J. *Biochem. J.* **2003**, *372*, 687–693.
- (11) Grummitt, A. R.; Rutledge, P. J.; Clifton, I. J.; Baldwin, J. E. *Biochem. J.* **2004**, *382*, 659–666.
- (12) Long, A. J.; Clifton, I. J.; Roach, P. L.; Baldwin, J. E.; Rutledge, P. J.; Schofield, C. J. *Biochemistry* **2005**, *44*, 6619–6628.
- (13) Howard-Jones, A. R.; Rutledge, P. J.; Clifton, I. J.; Adlington, R. M.; Baldwin, J. E. *Biochem. Biophys. Res. Commun.* **2005**, *336*, 702–708.
- (14) Daruzzaman, A.; Clifton, I. J.; Adlington, R. M.; Baldwin, J. E.; Rutledge, P. J. *ChemBioChem* **2006**, *7*, 351–358.
- (15) Howard-Jones, A. R.; Elkins, J. M.; Clifton, I. J.; Roach, P. L.; Adlington, R. M.; Baldwin, J. E.; Rutledge, P. J. *Biochemistry* **2007**, *46*, 4755–4762.

intermediate. We report herein the use of ACOmC in further crystallographic studies of the IPNS reaction mechanism.

## Results and Discussion

### Structure of the Anaerobic IPNS/Fe(II)/ACOmC Complex.

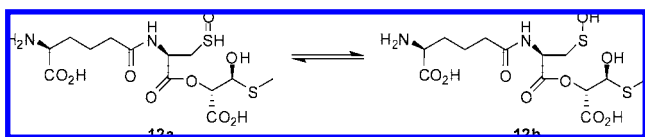
ACOmC **11** was synthesized and crystallized anaerobically with IPNS and Fe(II). The crystal structure of the IPNS/Fe(II)/ACOmC complex was solved to a resolution of 1.80 Å (Figure 1a). ACOmC binds in a similar manner to ACV, being tethered by a salt bridge to Arg87, by hydrogen bonding to Tyr189, Arg279, and Ser281, and to the iron atom through its cysteinyl sulfur.

The iron is pentacoordinate in the IPNS/Fe(II)/ACV complex, but in this new structure, the metal is hexacoordinate and the sulfur of the *S*-methyl sulfide is bound in the proposed oxygen binding site *trans* to Asp216. The coordination of ACOmC to the iron is very similar to that observed for ACmC.<sup>6</sup> The *S*-methyl sulfur–iron bond length is 2.69 Å, and the cysteinyl sulfur–iron distance, 2.45 Å. In the ACV complex, the cysteinyl sulfur–iron distance is 2.41 Å, while in the IPNS/Fe(II)/ACmC complex the cysteinyl sulfur–iron bond is also 2.41 Å, and the methylsulfide sulfur–iron bond is 2.69 Å. The IPNS/Fe(II)/ACOmC complex differs from the IPNS/Fe(II)/ACmC structure in the bond angle between the second and third residues: the C–NH–C angle in ACmC is 121.6°, while the C–O–C angle in ACOmC is 118.5°.

**Structure of the IPNS/Fe(II)/ACOmC Complex after Exposure to Oxygen.** Despite the positioning of the sulfide in the putative oxygen binding site, the IPNS/Fe(II)/ACOmC complex is turned over on exposure to high-pressure oxygen. Crystals of the IPNS/Fe(II)/ACOmC complex were exposed to high pressures of oxygen using a wide range of conditions. Pressurization for 35 min at 40 bar proved optimal. The resulting X-ray structure was solved to a resolution of 1.50 Å (Figure 1b,c).

There are two significant changes in the electron density map of the structure after exposure to oxygen: an extension of electron density around the cysteinyl sulfur atom, pointing toward the iron, and additional density adjacent to the  $\beta$ -carbon of the thiomethyl-propanoate residue. These changes are consistent with the formation of a metal-bound sulfenate product **12**, which is hydroxylated at the  $\beta$ -carbon of the third residue (Scheme 3). In a third, more minor change, the methyl carbon of the thiomethyl group exhibits some disorder and has been modeled in two occupancies.

**Scheme 3.** Structure of the Oxidized Product Formed upon High-Pressure Turnover of ACOmC in the Active Site of Crystalline IPNS



The sulfenate moiety of **12** appears to coordinate side-on to Fe(II) in the IPNS active site. This is a similar binding mode to that previously observed in several small-molecule complexes of sulfenates with first-row transition metals. For example Kovacs and co-workers have reported a cobalt(III) complex with side-on-bound sulfenate in their investigation of nitrile hydratase

mimetics,<sup>17</sup> and Cornman *et al.* have prepared a vanadium(V) complex incorporating a similar mode of sulfenato ligation.<sup>18</sup>

The additional density around C $\beta$  of the thiomethyl-propanoate side chain is consistent with hydroxylation at this position. IPNS has previously been shown to effect hydroxylation of various tripeptide substrates *via* several mechanisms,<sup>3,8,9,14</sup> while other nonheme iron(II) dependent oxidases mediate oxygen insertion into a range of aliphatic C–H bonds in reactions generally thought to involve high-valent iron intermediates.<sup>19–25</sup> There is therefore considerable precedent for hydroxylation reactions of this type.

**A Mechanism for Product Formation.** The observed formation of the sulfenate product **12** suggests that ACOmC follows a different pathway even in the initial stage of its reaction with IPNS. In the reaction of IPNS with ACV (and numerous analogues studied previously), it is thought that dioxygen binds to iron in the site opposite Asp216 and then abstracts one hydrogen from the cysteinyl  $\beta$ -carbon to afford a thioaldehyde **4** (Scheme 1). However, in the reaction of ACOmC the hydrogen atoms on the cysteinyl C $\beta$ -carbon appear to escape the reaction cycle unscathed, suggesting that the mechanism must diverge at a very early stage from that seen with the natural substrate. A plausible mechanism for the oxidation of ACOmC by IPNS must explain why the reaction diverges from the path of ACV turnover at the earliest stage, i.e. why C–H abstraction from the cysteinyl C $\beta$  is not observed.

Two significant differences are evident in the anaerobic IPNS/Fe(II)/ACOmC complex relative to the corresponding ACV complex.<sup>5</sup> First, the IPNS complex with ACOmC **11** shows a C–O–C ester bond angle that is smaller than the amide C–NH–C angle seen in complexes of IPNS with tripeptides such as ACV and ACmC: the C–O–C bond angle in ACOmC is 118.5°, versus a C–NH–C angle in ACmC of 121.6°. Similar “narrowing” of this angle has been previously observed with other ester analogues,<sup>14</sup> and it brings about a slight shrinking of the pocket *trans* to Asp216. Second, the *S*-methyl group of the third ACOmC residue binds to iron in the site opposite Asp216, thus occupying the proposed site of oxygen binding.

There has been considerable debate over the position of oxygen binding to iron in IPNS, whether it binds opposite Asp216 or *trans* to His214, displacing the water ligand in the process.<sup>5,6</sup> Various structural data recorded to date supports the former binding site, with the IPNS/Fe(II)/ACV/NO structure offering particularly compelling evidence.<sup>5</sup> In previously reported complexes in which only one of the above conditions is established (i.e., either an *S*-methyl group occupying the site opposite Asp216 as in ACmC<sup>6</sup> or the ester link within the substrate analogue as for ACOV),<sup>8,14</sup> C–H abstraction from the cysteinyl C $\beta$  is observed; i.e. oxygen can still bind *trans* to

(16) Stewart, A. C.; Clifton, I. J.; Adlington, R. M.; Baldwin, J. E.; Rutledge, P. J. *ChemBioChem* **2007**, *8*, 2003–2007.

(17) Kung, I.; Schweitzer, D.; Shearer, J.; Taylor, W. D.; Jackson, H. L.; Lovell, S.; Kovacs, J. A. *J. Am. Chem. Soc.* **2000**, *122*, 8299–8300.

(18) Cornman, C. R.; Stauffer, T. C.; Boyle, P. D. *J. Am. Chem. Soc.* **1997**, *119*, 5986–5987.

(19) Zhang, Z.; Ren, J. S.; Stammers, D. K.; Baldwin, J. E.; Harlos, K.; Schofield, C. J. *Nat. Struct. Biol.* **1999**, *7*, 127–133.

(20) Prescott, A. G.; Lloyd, M. D. *Nat. Prod. Rep.* **2000**, *17*, 367–383.

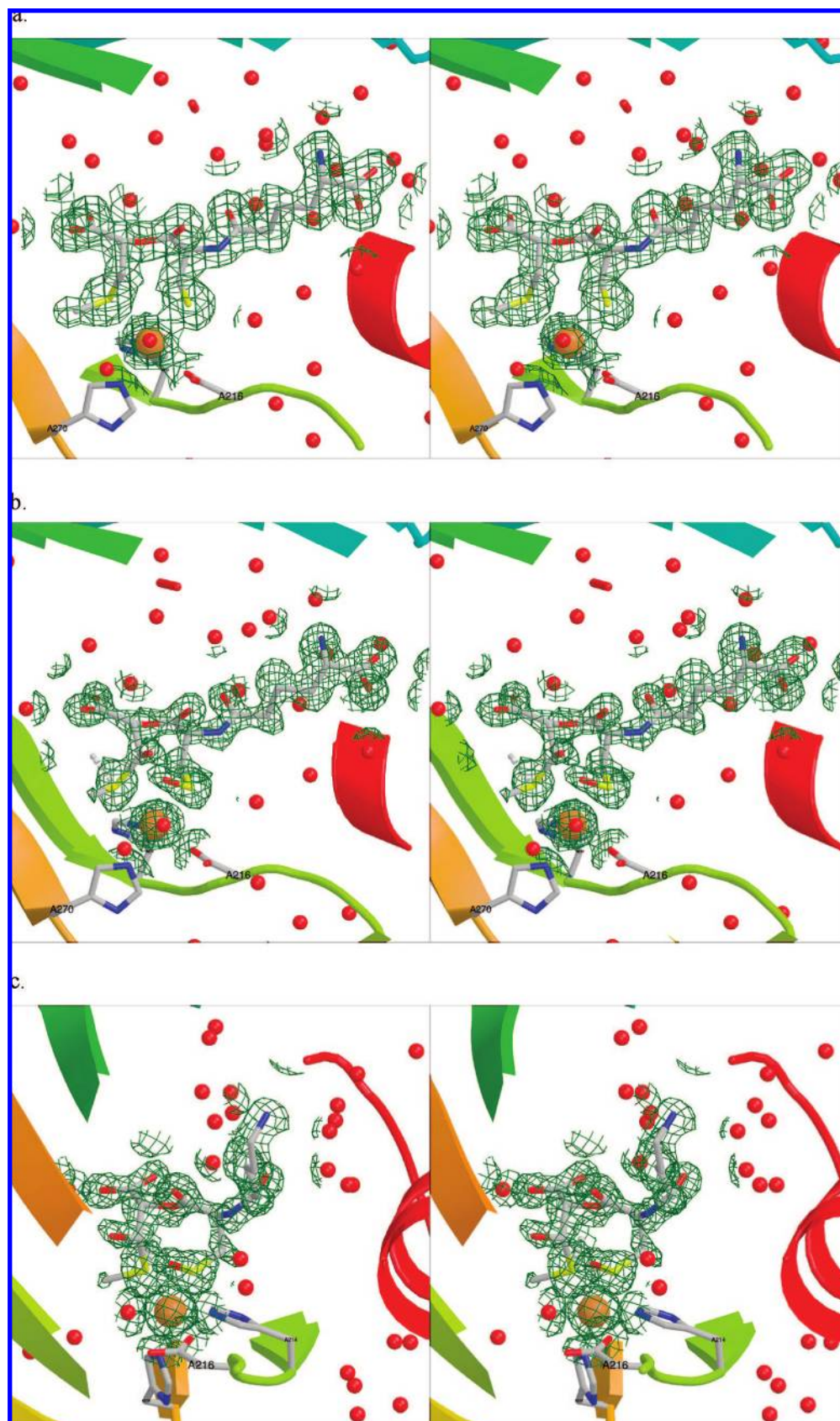
(21) Clifton, I. J.; Hsueh, L. C.; Baldwin, J. E.; Harlos, K.; Schofield, C. J. *Eur. J. Biochem.* **2001**, *268*, 6625–6636.

(22) Ryle, M. J.; Hausinger, R. P. *Curr. Opin. Chem. Biol.* **2002**, *6*, 193–201.

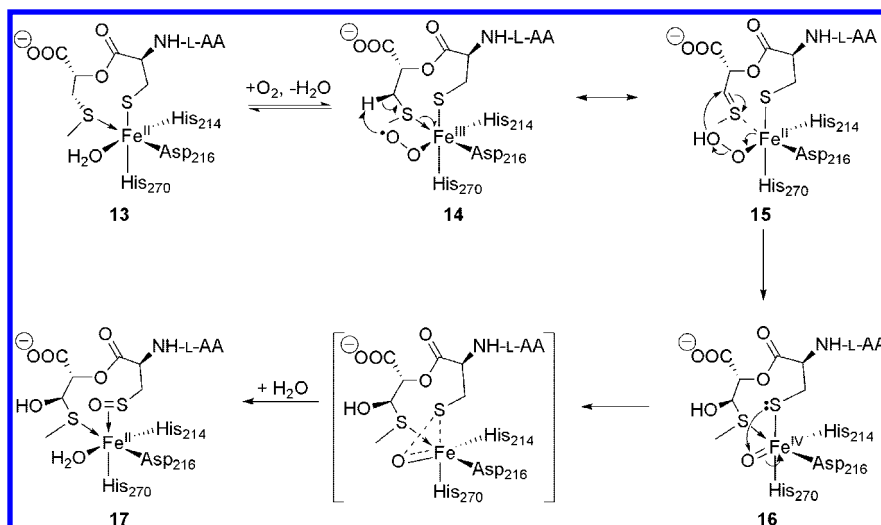
(23) Hausinger, R. P. *Crit. Rev. Biochem. Mol. Biol.* **2004**, *39*, 21–68.

(24) Costas, M.; Mehn, M. P.; Jensen, M. P.; Que, L. *Chem. Rev.* **2004**, *104*, 939–986.

(25) Koehntop, K. D.; Emerson, J. P.; Que, L. *J. Biol. Inorg. Chem.* **2005**, *10*, 87–93.



**Figure 1.** (a) Active site of anaerobic IPNS/Fe(II)/ACOMc complex. (b) IPNS/Fe(II)/ACOMc structure after 35 min under an oxygen pressure of 40 bar. The *S*-methyl group of the substrate's third residue is shown in two conformations: the first as a solid bond to a black carbon atom, the second as a dashed bond to a gray carbon atom. (c) Alternative representation of the oxygen-exposed IPNS/Fe(II)/ACOMc structure showing the hydroxyl group on the thiomethyl-propanoyl  $C\beta$  and the sulfonate oxygen atom; the two conformations occupied by the *S*-methyl group are represented as in part 1b. In all images, the electron density map ( $2mF_o - DF_c$  map) is shown in green at  $1\sigma$ , the substrate/product is colored gray (carbon), blue (nitrogen), red (oxygen), and yellow (sulfur), iron is orange, and water molecules are shown as red spheres.

**Scheme 4.** Proposed Mechanism for the Formation of the Hydroxylated Sulfenic Acid Product **12** from ACOmC **11****Table 1.** X-ray Data Collection and Crystallographic Statistics; Both Crystals of IPNS/Fe(II)/ACOmC

oxygen exposure	unexposed	35 min, 40 bar		
X-ray source	Strubi, Oxford	Beamline 14.2 SRS		
wavelength	1.5418	0.9795		
PDB code	2vau	2vbb		
resolution (Å)	1.80	1.40		
space group	$P2_12_12_1$	$P2_12_12_1$		
unit cell ( $a-c$ , Å)	46.70, 71.16, 100.91	46.65, 71.04, 100.76		
total reflections	287 147	439 749		
resolution shell (Å)	34.0–1.80	1.90–1.80	27.0–1.40	1.48–1.40
unique reflections	31 926	2265 <sup>c</sup>	66 244	4445 <sup>d</sup>
average $I/\sigma(I)$	21.0	7.2	17.0	2.9
completeness (%)	98.4	89.0	99.3	95.1
$R_{\text{merge}}^a$	9.7	27	7.4	50
$R_{\text{cryst}}^b$ (%)	15.1	17.4 <sup>c</sup>	15.2	24.1 <sup>d</sup>
$R_{\text{free}}^e$ (%)	18.9	20.8 <sup>c</sup>	17.2	25.1 <sup>d</sup>
rms deviation <sup>f</sup>	0.02 (1.7)	0.03 (2.6)		
$B$ factors (Å <sup>2</sup> ) <sup>g</sup>	10, 12, 7, 21	6, 8, 14, 28		
water molecules	345	447		

<sup>a</sup>  $R_{\text{merge}} = \frac{\sum_i \sum_j |I_{ij} - \langle I_i \rangle|}{\sum_i \sum_j \langle I_i \rangle} \times 100$ . <sup>b</sup>  $R_{\text{cryst}} = \frac{\sum |F_{\text{calc}} - F_{\text{obs}}|}{\sum |F_{\text{obs}}|} \times 100$ . <sup>c</sup> For outer shell of 1.85–1.80 Å. <sup>d</sup> For outer shell of 1.44–1.40 Å. <sup>e</sup>  $R_{\text{free}}$  = based on 4% of reflections. <sup>f</sup> rms deviation from ideality for bonds (followed by the value for angles). <sup>g</sup> Average  $B$  factors in order: main chain, side chain, substrate, and solvent.

Asp216 and launch the “standard” mode of initial reaction with this cysteinyl  $C\beta$ –H. However it seems that in the particular case of ACOmC, with two sulfurs bound to iron and the ester link further changing the geometry, oxygen cannot gain entry to bind at its “normal” site opposite Asp216, close to the cysteinyl  $\beta$ -carbon. Under these circumstances, it seems plausible that oxygen could bind at a different position on the metal, displacing the water ligand and ligating *trans* to His214. This would position the resulting superoxide species much closer to the propanoyl  $C\beta$ –H than to the cysteinyl  $C\beta$ –H and facilitate a different  $C\beta$ –H extraction (Scheme 4). The stereochemistry of the new hydroxyl group at the propanoyl  $C\beta$  in product **12** is consistent with oxygen attack from a position “in front” of iron, as would occur if dioxygen bound opposite His214.

Thus we propose the following mechanism to explain the IPNS-mediated formation of **12** from ACOmC **11**. First ACOmC binds in the IPNS active site, displacing Gln330 to form the anaerobic complex **13** in which both sulfur atoms from the substrate bind to iron (as seen in Figure 1a). Sulfur binding

reduces the Fe(III)/Fe(II) redox potential, facilitating coordination of molecular oxygen to give **14**. In contrast to the reaction of ACV (Scheme 1), we postulate that oxygen binds *trans* to His214 displacing the water ligand from this site, for the reasons discussed above. A superoxide species bound in this position would be too remote to react with the cysteinyl  $C\beta$ –H and could instead abstract the chemically similar  $C\beta$ –H of the propanoyl residue to form **15**. The resulting hydroperoxide moiety could then act as a nucleophile and attack the thioaldehyde-like  $\beta$ -carbon of the propanoyl residue, hydroxylating at that position and forming an Fe(IV)-oxo species **16**. This reactive intermediate could then be intercepted by the cysteinyl sulfur (unreacted until this point) to generate the observed sulfenate complex **17** (after re-entry of a water ligand).

It is possible to conceive of a reaction *via* initial oxygen binding *trans* to Asp216. However, such a mechanism does not readily explain why the resulting iron-bound superoxide does not then abstract the cysteinyl  $C\beta$ –H as it does in the reaction with ACV (Scheme 1) or ACmC but reacts instead with the cysteinyl sulfur atom or propanoyl  $C\beta$ –H. By this alternative mechanism for the formation of **12** (presented in full in the Supporting Information), oxygen binding opposite Asp216 could be followed by direct attack of superoxide on the cysteinyl sulfur (prompted perhaps by the subtly different nature of the active site region in the IPNS/Fe(II)/ACOmC complex). Water-mediated cleavage of the O–O bond would afford an Fe(IV)-oxo intermediate, which could then hydroxylate the propanoyl  $\beta$ -carbon to yield the observed product complex **17**.

## Conclusion

Crystallization of IPNS with the substrate analogue ACOmC **11** and turnover of the crystalline enzyme–substrate complex reveals yet more interesting oxidative chemistry mediated by this remarkable enzyme. This particular substrate analogue binds at the IPNS active site in such a way that the cosubstrate, dioxygen, appears unable to coordinate at its usual binding site opposite Asp216 and ligates instead opposite His214. This opens an alternative mode of oxidative reaction to hydroxylate the third residue of the depsipeptide analogue and directly oxidize the iron-bound thiolate of the cysteine residue. This has afforded the first crystal structure of a sulfenate species coordinated to iron at the IPNS active site.

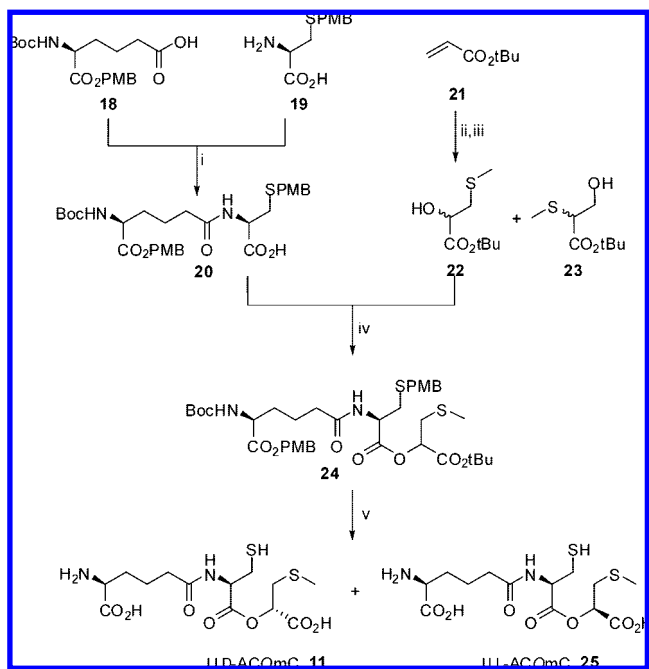
The apparent binding of oxygen opposite His214 in the IPNS/Fe(II)/ACOMC complex necessitates further consideration of the proposed oxygen binding site in the IPNS/Fe(II)/ACV complex. Based on the IPNS/Fe(II)/ACV/NO structure and the proposed initial steps of ACV turnover, it has become widely accepted that oxygen binds to iron opposite Asp216 in the IPNS/Fe(II)/ACV complex. While the current study indicates oxygen binding to a different position in the IPNS/Fe(II)/ACOMC complex, this is most likely due to the specific combination of electronic and steric factors at play in this complex (as discussed above). Thus a more general revision of oxygen binding to IPNS/Fe(II)/substrate complexes is not in order.

The oxygen-mediated conversion of an iron-bound thiolate to a sulfenate reported here is of particular interest when considered in the context of the distantly related nonheme iron enzymes nitrile hydratase (NHase)<sup>26,27</sup> and thiocyanate hydratase.<sup>28</sup> These metalloenzymes mediate the addition of water to nitrile and thiocyanate substrates, respectively, and incorporate a most unusual metal-binding motif at their nonheme iron(III) or noncorrinoid cobalt(III) active site. In these proteins, two nitrogen ligands derived from main-chain amides and three differently oxidized sulfur atoms are coordinated to the metal center. The three cysteine-derived sulfur ligands are a thiolate, a sulfenate (SO), and a sulfinate (SO<sub>2</sub>). The timing and mechanism of the post-translational oxidation that affords this unusual ligand set are not fully understood, but it is essential for activity: NHase assembled in an anaerobic environment shows no catalytic activity and is reactivated upon aerobic incubation.<sup>29</sup> Moreover, modification to Cys-SO<sub>2</sub>H and Cys-SOH occurs concomitant with reactivation (as observed by mass spectrometry) and in the absence of other proteins.<sup>29</sup> “Self” oxidation of the cysteinyl thiolates by the active site metal appears a likely route to the sulfenato and sulfinato ligands at the nitrile hydratase active site, although there is as yet little direct evidence to support this theory. The IPNS-mediated oxidation of a metal-bound thiolate observed in this investigation offers a tantalizing “proof of concept” for the type of oxidation required at the nitrile hydratase active site and points to a possible link between IPNS and another important family of nonheme iron enzymes.

## Experimental Section

**Synthesis of ACOMC.** The suitably protected L- $\alpha$ -amino adipic acid derivative **18** and *S*-*p*-methoxybenzyl-L-cysteine **19** were coupled using *iso*-butylchloroformate methodology to afford dipeptide **20** (Scheme 5).<sup>30</sup> Epoxidation of *tert*-butyl acrylate **21** was achieved using the Prilezhaev reaction.<sup>31,32</sup> *tert*-Butyl (2-hydroxy-3-thiomethyl)propanoate **22** was obtained from the epoxide intermediate using sodium methanethiolate under basic conditions at 0 °C; the desired regioisomer **22** was separated from the regiois-

**Scheme 5.** Synthesis of Depsipeptide Substrate Analogue ACOMC 11<sup>a</sup>



<sup>a</sup> (i) **18**, *iso*-butylchloroformate, Et<sub>3</sub>N, THF, -12 °C, 30 min, then **19**, Et<sub>3</sub>N, H<sub>2</sub>O, 0 °C - RT, 90 min, 82%; (ii) *m*-CPBA, DCM, reflux, 48 h; (iii) NaSCH<sub>3</sub>, NaHCO<sub>3</sub>, H<sub>2</sub>O, 0 °C, 1 h, 80% (over two steps) of a 1:2 mixture of **22/23**; (iv) PPh<sub>3</sub>, DEAD, THF, 0 °C, sonication 1 h then RT 20 h, 63% of 1:1 mixture LLL/LLD-**24**; (v) TFA, anisole, reflux, 30 min then RP-HPLC (conditions in main text), 43% of LLD-ACOMC **11** + 36% of LLL-ACOMC **25**. Full synthetic procedures and characterization details are provided in the Supporting Information.

meric side product **23** by column chromatography. The protected depsipeptide **24** was obtained by coupling dipeptide **20** and alcohol **22** employing the Mitsunobu reaction.<sup>33</sup> Global deprotection of **24** using TFA and anisole<sup>34</sup> followed by reversed-phase HPLC purification (10 mM NH<sub>4</sub>HCO<sub>3</sub>, Hypersil 5  $\mu$  C18 column, 250 mm  $\times$  10 mm internal diameter;  $\lambda$  = 254 nm; 4 mL/min) afforded the pure, separated isomers: LLL-ACOMC **25** (*R*<sub>t</sub> = 12.8 min) and LLD-ACOMC **11** (*R*<sub>t</sub> = 13.5 min). Full experimental procedures and spectroscopic data for the synthesis of **11** are included in the Supporting Information.

**Crystallization and Turnover Experiments.** Crystals of the IPNS/Fe(II)/ACOMC complex were grown under anaerobic conditions as reported previously.<sup>35</sup> The crystals were subjected to rapid cryo-cooling in liquid nitrogen upon removal from the anaerobic environment. Thus a drop containing the crystals was removed from the glovebox, and the individual crystals were removed from the drop with the aid of a light microscope, soaked for *ca.* 5 s in cryoprotectant (1:1 mixture of well buffer: saturated Li<sub>2</sub>SO<sub>4</sub> in 40% (v/v) glycerol solution), mounted in loops, and cryo-cooled in liquid nitrogen to furnish samples ready for crystallographic analysis. These were stored in liquid nitrogen until required. Drops containing crystals for oxygen exposure experiments were removed from the glovebox, and then the glass microcoverslip was inverted and transferred to the high-pressure oxygen device and exposed to oxygen for the designated time as detailed previously.<sup>7</sup> Once exposed to oxygen the crystals were removed and frozen as above.

- (26) Huang, W. J.; Jia, J.; Cummings, J.; Nelson, M.; Schneider, G.; Lindqvist, Y. *Structure* **1997**, *5*, 691–699.  
 (27) Endo, I.; Nojiri, M.; Tsujimura, M.; Nakasako, M.; Nagashima, S.; Yohda, M.; Odaka, M. *J. Inorg. Biochem.* **2001**, *83*, 247–253.  
 (28) Katayama, Y.; Hashimoto, K.; Nakayama, H.; Mino, H.; Nojiri, M.; Ono, T.; Nyunoya, H.; Yohda, M.; Takio, K.; Odaka, M. *J. Am. Chem. Soc.* **2006**, *128*, 728–729.  
 (29) Murakami, T.; Nojiri, M.; Nakayama, H.; Odaka, M.; Yohda, M.; Dohmae, N.; Takio, K.; Nagamune, T.; Endo, I. *Protein Sci.* **2000**, *9*, 1024–1030.  
 (30) Baldwin, J. E.; Herchen, S. R.; Johnson, B. L.; Jung, M.; Usher, J. J.; Wan, T. *J. Chem. Soc., Perkin Trans. 1* **1981**, 2253–2257.  
 (31) Prilezhaev, N. *Ber. Deut. Chem. Ges.* **1910**, *42*, 4811–4815.  
 (32) Hagen, T. J. In *Name Reactions for Functional Group Transformations*; Li, J. J., Corey, E. J., Eds.; John Wiley & Sons, Inc.: Hoboken, NJ, 2007; pp 274–281.

- (33) Mitsunobu, O. *Synthesis-Stuttgart* **1981**, 1–28.  
 (34) Bodanzky, M.; Bodanzky, A. In *Reactivity and Structure Concepts in Organic Chemistry*; Hafner, K., Rees, C. W., Trost, B. M., Lehn, J. M., Schleyer, P. v. R., Zahruchik, R., Eds.; Springer-Verlag: Berlin, 1984; Vol. 21, pp 172–173.  
 (35) Roach, P. L.; Clifton, I. J.; Hensgens, C. M. H.; Shibata, N.; Long, A. J.; Strange, R. W.; Hasnain, S. S.; Schofield, C. J.; Baldwin, J. E.; Hajdu, J. *Eur. J. Biochem.* **1996**, *242*, 736–740.

**Data Collection and Structure Determination.** Data were collected at 100 K using either the Cu K $\alpha$  radiation from a Rigaku rotating anode generator and a 300 mm MAR Research image plate detector at the Division of Structural Biology (STRUBI) of the Wellcome Trust Centre for Human Genetics at the University of Oxford, UK (anaerobic IPNS/Fe(II)/ACOmC complex) or synchrotron radiation and an ADSC CCD detector at Beamline 14.2 of the Synchrotron Radiation Source (SRS), Daresbury, U.K.

Data were processed using MOSFLM<sup>36</sup> and programs from the CCP4 suite.<sup>37</sup> Refinement was carried out using REFMAC5,<sup>38</sup> and the program O was used for model building.<sup>39</sup> Initial phases were generated by molecular replacement, using coordinates for the protein from the IPNS/Fe(II)/ACV structure published previously. Manual rebuilding of protein side chains was performed as necessary. Crystallographic coordinates and structure factors have

been deposited in the Worldwide Protein Data Bank, accession numbers 2vau for the anaerobic IPNS/Fe(II)/ACOmC structure and 2vbb for the oxygen-exposed IPNS/Fe(II)/ACOmC complex.

Color figures were prepared using the programs MOLSCRIPT,<sup>40</sup> BOBSCRIPT,<sup>41</sup> and Raster3D.<sup>42</sup>

**Acknowledgment.** We thank Dr. Annaleise Howard-Jones, Prof. Chris Schofield, Dr. Victor Lee, Dr. Zhihong Zhang, Dr. Karl Harlos, Dr. Jing He, and the scientists at SRS Daresbury for help and discussions.

**Supporting Information Available:** Details of the alternative mechanism for the formation of **12** from **11**, plus full synthetic procedures and spectroscopic data for the preparation of ACOmC **11** and scanned spectra for **11**. This information is available free of charge via the Internet at <http://pubs.acs.org>.

JA8005397

(36) Leslie, A. G. W. *Acta Crystallogr. D* **1999**, *55*, 1696–1702.

(37) Collaborative Computational Project Number 4. *Acta Crystallogr., D*, **1994**, *50*, 760–763.

(38) Murshudov, G. N.; Vagin, A. A.; Dodson, E. J. *Acta Crystallogr., Sect. D* **1997**, *53*, 240–255.

(39) Jones, T. A.; Zou, J. Y.; Cowan, S. W.; Kjeldgaard, M. *Acta Crystallogr., A* **1991**, *47*, 110–119.

(40) Kraulis, P. J. *J. Appl. Crystallogr.* **1991**, *24*, 946–950.

(41) Esnouf, R. M. *Acta Crystallogr., D* **1999**, *55*, 938–940.

(42) Merritt, E. A.; Bacon, D. J. *Methods Enzymol.* **1997**, *277*, 505–524.